Chinese Chemical Letters 36 (2025) 110039

Contents lists available at ScienceDirect

Chinese Chemical Letters

journal homepage: www.elsevier.com/locate/cclet

Recent research on aqueous zinc-ion batteries and progress in optimizing full-cell performance

Tong Peng[a,c,1], Yupeng Xing[a,b,1], Lan Mu[a,1], Chenggang Wang[a,*], Ning Zhao[a], Wenbo Liao[a], Jianlei Li[d], Gang Zhao[a,*]

[a] School of Physics and Technology, University of Jinan, Ji'nan 250022, China
[b] School of System Design and Intelligent Manufacturing, Southern University of Science and Technology, Shenzhen 518055, China
[c] Institute of Novel Semiconductors, State Key laboratory of Crystal Material, Shandong University, Ji'nan 250100, China
[d] Weifang Special Equipment Inspection and Research Institute, Weifang 261000, China

ARTICLE INFO

Article history:
Received 23 March 2024
Revised 28 April 2024
Accepted 22 May 2024
Available online 23 May 2024

Keywords:
Aqueous zinc-ion batteries
Energy storage mechanism
Cathode materials
Zinc anode
Electrolyte
Full battery optimization

ABSTRACT

With the development of science and technology, there is an increasing demand for energy storage batteries. Aqueous zinc-ion batteries (AZIBs) are expected to become the next generation of commercialized energy storage devices due to their advantages. The aqueous zinc ion battery is generally composed of zinc metal as the anode, active material as the cathode, and aqueous electrolyte. However, there are still many problems with the cathode/anode material and voltage window of the battery, which limit its use. This review introduces the recent research progress of zinc-ion batteries, including the advantages and disadvantages, energy storage mechanisms, and common cathode/anode materials, electrolytes, *etc*. It also gives a summary of the current research status of each material and provides solutions to the problems they face. Finally, it looks at the future direction and methods to optimize the performance of zinc-ion full batteries.

1. Introduction

As mentioned above, non-aqueous LIBs have advantages such as large specific capacity and long cycle life and have become the mainstream energy storage system in fields such as mobile electronic devices and emerging oil-electric hybrid vehicles. However, the current scarcity of lithium resources, high price, and serious safety hazards have seriously restricted the scale application of LIBs in power stations and other sites with high safety levels. In other new types of batteries, because sodium, potassium and lithium are the same main group elements with similar chemical structures, and abundant reserves and low prices, sodium and potassium have the potential to become new energy materials to replace lithium. However, sodium ion batteries (SIBs) and potassium ion batteries (KIBs) still have the problems of low energy density and high operating costs, and the organic electrolyte of these batteries has increased safety risks for the practical application of the batteries because of its highly toxic and flammable nature. Therefore, the use of aqueous batteries instead of batteries with organic electrolytes not only helps to improve the stability of the energy storage system, but also to obtain a more cost-effective battery device. Zinc is abundant, has low toxicity compared to lithium and is the most energetic of the metal elements that can be stabilized in aqueous solution [1], as well as having the advantages of a low balance potential and a high overpotential for hydrogen reaction. Due to its superior properties such as reliable safety, absence of any risk of flame or explosion, great cost competitiveness, eco-friendliness, high theoretical capacity, and long-term cyclic stability, it is expected to be used in large scale in various energy storage systems in the future.

Among aqueous secondary batteries, zinc-based batteries are the most promising energy storage system in recent years. As the negative electrode of zinc-based batteries, metallic zinc has low potential (−0.76 V *vs.* NHE), abundant reserves, and is green and non-toxic. Its redox involves a two-electron reaction and has the highest volumetric energy density (5855 mAh/cm^3) among aqueous electrode materials. Compared with strongly acidic lead-acid batteries and strongly alkaline nickel-metal hydride batteries, zinc-based batteries mostly use mild weak acid or neutral electrolytes, which greatly reduces the corrosion resistance requirements for battery parts such as the collector and shell. Moreover, the aque-

* Corresponding authors.
E-mail addresses: sps_wangcg@ujn.edu.cn (C. Wang), sps_zhaog@ujn.edu.cn (G. Zhao).
[1] These authors contributed equally to this work.

https://doi.org/10.1016/j.cclet.2024.110039
1001-8417/

ous electrolyte is inexpensive, and the batteries can be assembled directly in the air environment, so it has a significant advantage in cost. In addition, zinc anode can be flexibly paired with a variety of cathodes, such as zinc-ion batteries with solid embedded-type materials, zinc-liquid-flow batteries with liquid soluble molecules, and zinc-air batteries with gas cathodes; this makes zinc-based batteries have a huge energy enhancement potential. Among them, aqueous zinc-ion batteries are highly reversible and the most rapidly developing and are regarded as strong candidates for various power sources. Zinc-ion batteries have the following advantages:

(1) Good multiplier performance. When the current density is small, the charging and discharging rate is slow; on the contrary, when the current density is large, the charging and discharging rate is fast. Under very large current conditions, the reversible charge and discharge process of zinc-ion battery is only a few tens of seconds [2,3]. Since zinc-ion batteries can complete charging and discharging in a short period of time, they have a promising application in many places where fast charging and discharging are required.
(2) Environmental protection, safety, and reliability. The electrolyte of zinc-ion batteries generally adopts zinc sulfate, zinc acetate aqueous solution, which has the advantages of non-toxic and non-flammable, with a pH close to neutral, and is more environmentally friendly than the highly toxic and flammable organic electrolyte [4-6]. No pollutants are generated during the production and use of the battery, causing minimal impact on the environment.
(3) Low price and simple process. Zinc metal resources are abundant, the raw material is easily available, the preparation difficulty is low, which reduces the production cost; furthermore, the battery can be assembled in the air, and the manufacturing process is simple. Low-priced raw materials and simple production methods make the production cost of zinc-ion batteries lower than other types of batteries, and more advantageous in the promotion and application [7-9].
(4) High theoretical energy density and power density. Comparing the performance of zinc-ion batteries (ZIBs) with other existing small portable energy devices, it is found that: zinc-ion batteries have high power density as well as high energy density, which can not only be discharged slowly under low-power conditions, like ordinary batteries, but also complete charging and discharging rapidly under high-power conditions, like supercapacitors, thus possessing the advantages of both at the same time [10].

Despite the above many advantages, the actual energy density and insufficient cycle life of aqueous zinc-ion batteries are still restricting their development at this stage. Due to the narrow thermodynamic stability window of water, the voltage of zinc-ion batteries is limited, and their charging and discharging processes are always coupled with the occurrence of side reactions such as hydrogen and oxygen precipitation. Meanwhile, it is highly influenced by the nature of electrolyte such as pH and additives, which leads to the complexity of the actual electrochemical behavior inside the battery and the unclear energy storage mechanism [11,12]. Consequently, the current development of zinc-ion batteries is confronted with the following difficulties: (1) Zinc anodes store energy through their own dissolution and deposition. They are similarly susceptible to dendrite formation during deposition, which can lead to short circuits [13,14]. (2) The majority of cathode materials exhibit a relatively low voltage plateau and are structurally unstable, prone to electrode degradation [15,16]. (3) The existing zinc storage anode materials have limited capacity, and the large polarization of divalent zinc ions slows down the kinetic processes of embedding and detachment, while destroying the structural stability of the anode material, which results in poor multiplicative performance of the battery [17-19]. (4) The electrolyte of zinc-ion batteries can be either acidic or alkaline. The occurrence of by-product reactions such as hydroxide precipitation will lead to significant changes in the local pH value, in comparison with lithium-ion batteries. This places higher requirements on the acid and alkali corrosion resistance of the diaphragm. (5) In practical outdoor use, the solidification of aqueous electrolytes at low temperatures and volatilization at high temperatures will accelerate the degradation of device performance [20].

Therefore, in this review, we will start from the energy storage mechanism of zinc-ion batteries, elaborate the comparison, summarize, and analyze the energy storage mechanism of several kinds of zinc-ion batteries in detail, and then list and classify the current development status of zinc-ion batteries' anode and cathode materials, and encountered problems and the optimal solution methods. Besides, we will introduce the research status of electrolytes, and summarize the improvement methods of common types of electrolytes, aiming to make it easier for everyone to search for them. Eventually, the above aspects are summarized, and the development direction is expected (Fig. 1). This review of zinc-ion batteries will play a role in the development of zinc-ion batteries.

2. Energy storage mechanism of zinc-ion batteries

The reaction mechanism of aqueous zinc-ion batteries is controversial and has many issues compared to the reaction mechanisms of other ion batteries for energy storage. In particular, the reaction mechanism involving the energy storage process has been the focus of discussion and controversy. According to the available research papers, several reaction mechanisms have been proposed for aqueous zinc-ion batteries, including the traditional Zn^{2+} insertion/deinsertion, dual-ion co-insertion mechanism, the chemical conversion reaction theory, and the coordination reaction of Zn^{2+} with structural organic framework cathode materials and other mechanisms (Figs. 2a–d) [21-24]. The general categorization of the energy storage mechanisms of zinc-ion batteries and their specific reaction mechanisms and corresponding representative electrode materials will be described in detail in the following sections.

2.1. Zn^{2+} detachment/insertion mechanism

The Zn^{2+} detachment/insertion mechanism proposed earlier is the most common energy storage mechanism, similar to that of lithium-ion and sodium-ion batteries [1,21]. During working discharge, the anode loses electrons and Zn^{2+} is embedded in the cathode active material after entering the electrolyte as a carrier, and the cathode receives electrons as the oxidation state decreases; when the battery is charged, the anode material is dissolved in the electrolyte in the form of Zn^{2+}, and electrons are obtained by the external circuit to be reduced to metallic Zn and deposited onto the anode (Fig. 3a) [25]. This process can be summarized in a general equation as follows:

$$\text{Anode reaction: } Zn \Leftrightarrow Zn^{2+} + 2e^- \quad (1)$$

$$\text{Cathode reaction: } M + xZn^{2+} + 2xe^- \Leftrightarrow Zn_xM \quad (2)$$

$$\text{Total reaction: } xZn + M \Leftrightarrow Zn_xM \quad (3)$$

wherein M is the cathode material. Materials with tunneling, layered or open-framework structures with sufficient space to accommodate Zn^{2+} are considered ideal cathode materials for ZIBs [10]. For example, the multistructured α-MnO_2 material was proposed

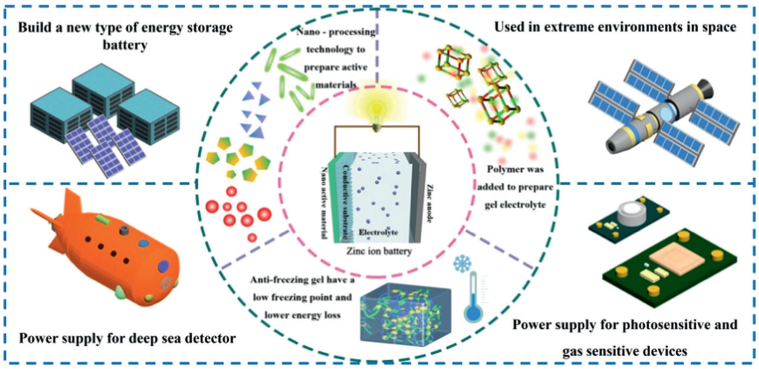

Fig. 1. Schematic diagram of the optimization scheme and application scenarios for aqueous zinc-ion batteries.

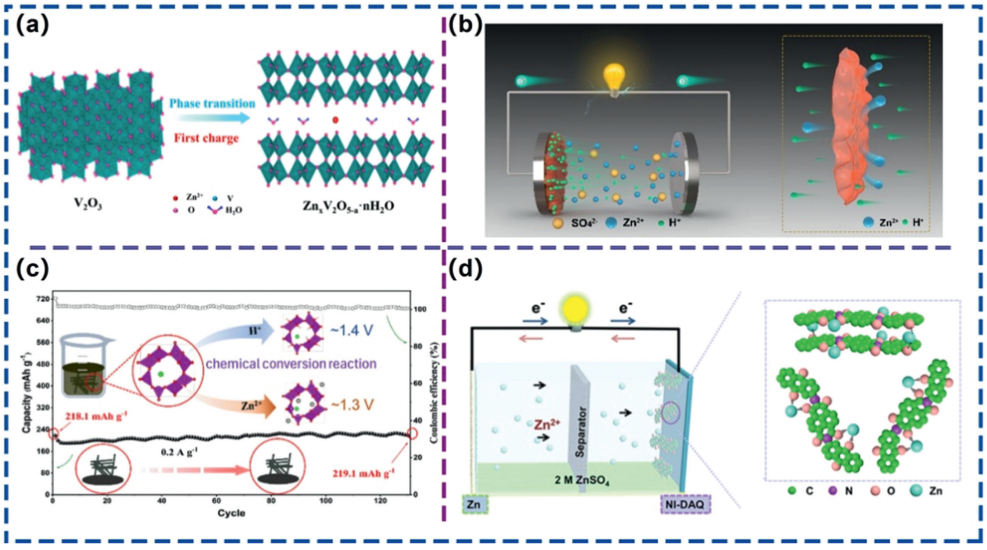

Fig. 2. (a) Phase transition conversion mechanism for an electrode material of V_2O_3@C. Reproduced with permission [21]. Copyright 2023, American Chemical Society. (b) Schematic diagram of the dual-ion insertion mechanism for MON-coated MnO_2-Zn cells. Reproduced with permission [22]. Copyright 2023, American Chemical Society. (c) Schematic diagram of the chemical conversion reaction energy storage mechanism for KMO nanorod cathodes. Reproduced with permission [23]. Copyright 2023, American Chemical Society. (d) NI-DAQ organic anode zinc-ion coordination mechanism. Reproduced with permission [24]. Copyright 2023, American Chemical Society.

by Feiyu Kang's team at Tsinghua University to reversibly insert Zn^{2+} will be inserted into the α-MnO_2 cathode/release from the α-MnO_2 cathode into the electrolyte during the discharge/charge of aqueous rechargeable zinc-ion [26]. This principle is quite different from the two-step energy storage mechanism of conventional alkaline zinc-manganese batteries. Subsequently, professor Yanbing He's team also demonstrated that the Zn^{2+} detachment/insertion mechanism occurs in β, γ, λ, δ and other types of MnO_2. At the same time, dissolution/deposition behaviors occur on the zinc metal anode side. In alkaline conditions, the surface of metallic zinc anode is prone to passivation to generate zinc oxide passivation, and prone to generate dendrites to make the zinc electrode utilization reduced, which is not conducive to the cyclic energy storage of zinc-ion batteries [27].

2.2. Dual-ion co-insertion mechanism

When Zn^{2+} is embedded, the phenomenon of slow embedding of zinc ion is often encountered, which is due to the large scale and high spatial resistance of zinc ion after hydration, and it carries a 2-unit positive charge, which makes a strong electrostatic repulsive force between it and the positive electrode material, and this repulsive force is able to impede the embedding of Zn^{2+}, which leads to the degradation of the performance of the battery. In fact, the insertion of zinc ions is allowing the host material to simultaneously insert other ions with higher diffusion kinetics (*e.g.*, H^+, Li^+, Na^+) [28], which can promote the effective utilization of the active sites on the structure of the host material and improve the energy storage of the battery. Yin *et al.* synthesized Mn_3O_4 electrode materials using MOF with a multidimensional laminate structure, and the process of H^+ and Zn^{2+} embedding was comprehensively explored by kinetic analysis and *ex situ* X-ray diffraction (XRD)/X-ray photoelectron spectroscopy (XPS) characterization [29]. Fig. 3b recorded the CV curves for the second cycle of Mn_3O_4@C electrode in the range of 0.8–1.9 V at 0.1 mV/s. During the anodic process, a strong oxidation peak at 1.62 V and an inconspicuous shoulder peak at 1.57 V can be attributed to the co-desorption reaction of Zn^{2+} and H^+. Fig. 3c showed the GCD curves of Mn_3O_4@C at different current densities from 0.2 A/g to 3 A/g. The gradual steepening of the discharge plateau with increasing current density indicates that the charge storage mechanism of the material is mainly controlled by the insertion/extraction process of Zn^{2+}.

2.3. Chemical transformation reaction theory

When investigating the above Zn ion embedding mechanism, the researchers found that when Zn ions were embedded during the discharge process, the concentration of cations of the positive material in the electrolyte increased instead, which was because

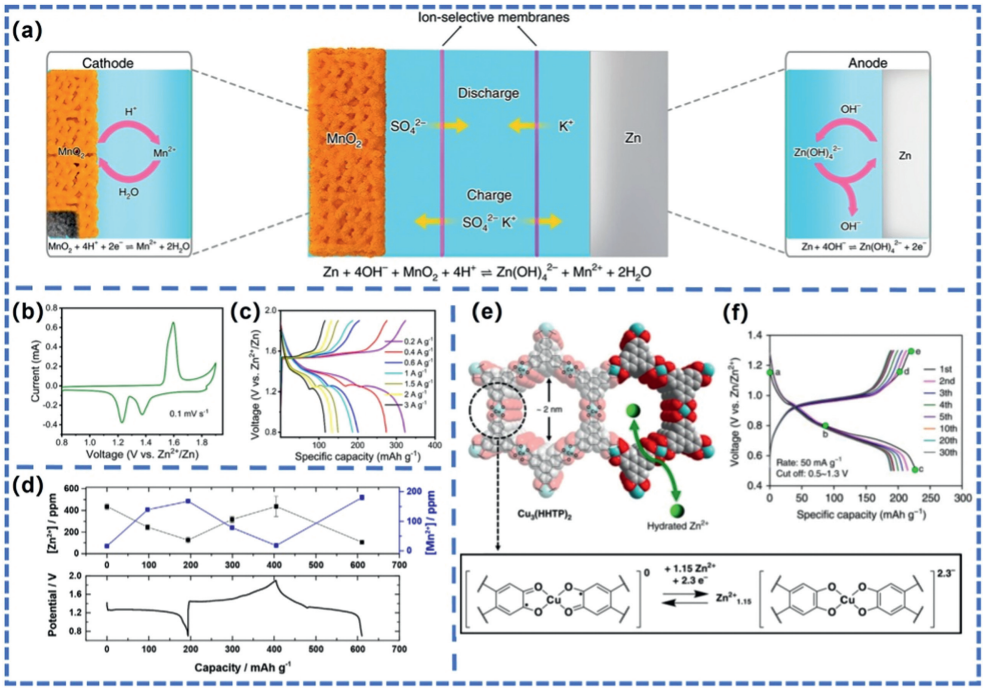

Fig. 3. (a) Working mechanism of the decoupling reaction in Zn-MnO_2 cells separated by a neutral electrolyte. Reproduced with permission [25]. Copyright 2020, Springer Nature Limited. Electrochemical properties of the Mn_3O_4@C cathode: (b) CV curve at a scan rate of 0.1 mV/s. (c) GCD curve at different current densities. Reproduced with permission [29]. Copyright 2022, American Chemical Society. (d) Zn (black squares) and Mn (blue squares) content in the electrolyte analysed by atomic absorption spectroscopy (AAS); corresponding discharge-charge curves of α-MnO_2/Zn cells. Reproduced with permission [30]. Copyright 2016, Chemistry Europe. (e) Structure of $Cu_3(HHTP)_2$; expected redox processes in the coordination unit of $Cu_3(HHTP)_2$. (f) discharge-charge voltage distribution of $Cu_3(HHTP)_2$ at 50 mA/g. Reproduced with permission [35]. Copyright 2019, Nature Publication Group.

the water in the aqueous electrolyte easily reacted with the active positive metal oxides to produce positively valent ions and hydroxides, such as MnO_2 positive $MnO_2 + 2H_2O + 2e^- \Leftrightarrow Mn^{2+} + 4OH^-$. As reported by Oh *et al.*, Fig. 3d showed that the concentration of Mn^{2+} tended to increase during discharge and decrease during charging, while the opposite was true for Zn^{2+} [30]. Such a small amount of Mn^{2+} detachment facilitates the embedding of Zn ions and promotes the migration rate of Zn ions, which increases the discharge rate of the battery, however, a large amount of dissolution of MnO_2 cathode destabilizes the cathode structure of the battery, which affects the cycling stability of charging and discharging. Yang *et al.* proposed a mild method for the batch synthesis of K-doped α-MnO_2 (KMO) nanorods and demonstrated that the zinc storage mechanism is mainly related to the chemical transformation reactions of H^+, Zn^{2+}, and MnO_2 of the KMO nanorods in the AZIBs by *in situ* XRD and DFT calculations [23].

More interestingly, it has been found that sometimes it is the H^+ that is embedded in the zinc-manganese battery rather than the Zn^{2+}. H^+ reacts with MnO_2 to form MnOOH, while Zn^{2+} combines with OH^- and then complexes with $ZnSO_4$ electrolyte to form zinc hydroxide sulfate ($ZnSO_4[Zn(OH)_2]_3{\cdot}12H_2O$) deposited on the surface of MnO_2. This embedded energy storage effect of H^+ is inferior to that of H^+ and Zn^{2+} co-embedded energy storage. Therefore, $MnSO_4$ is usually used as an additive in order to inhibit the reaction between MnO_2 and H^+ or the dissolution of MnO_2 cathode and to promote the cycling stability [5,31].

2.4. Coordination reaction of Zn^{2+} with structural organic framework cathode materials

Structural organic framework materials, such as MOF, COF, have both the lamellar, pore and three-dimensional open framework structures of common crystalline materials, and the advantages of organic polymers' structural and functional tunability enable them to provide abundant Zn^{2+} bonding sites; hence, in recent years, structural organic framework materials have also been frequently used as positive electrodes for zinc-ion batteries. These organic materials are diverse in their chemical composition, but the mechanism of zinc storage action is similar, mainly storing Zn^{2+} through coordination reactions, such as bonding with Zn^{2+} at positions such as quinone structures, neighboring C=O sites, and –NH functional groups [32-34]. We can facilitate the bonding embedding and embedding out of Zn ions by modifying the spacing of the coordination groups to accommodate the size of the Zn ions.

Metal-organic skeleton materials (MOFs) with conductive properties have received increasing research attention in the field of energy storage in ZIBs recently due to their tunable morphology, abundant active sites, and diverse functions. For example, Stoddart and colleagues employed a conductive two-dimensional metal-organic framework (MOF), $Cu_3(HHTP)_2$, with an open-framework structure analogous to that of the Prussian blue analog, as a high-performance cathode for rechargeable AZIBs. Density functional theory (DFT) calculations indicate that the quinone structure and copper in MOFs serve as redox centers. The $Cu_3(HHTP)_2$ cathode exhibits a rapid Zn^{2+} diffusion rate, low interfacial resistance, and high reversible capacity (Figs. 3e and f) [35]. Additionally, a vanadium-based metal–organic framework (MOF) material (MIL-47, V-MOF) has been identified as a cathode material for ZIBs with exceptional performance due to its excellent structural reversibility, which facilitates the de-embedding of Zn^{2+} [36]. Moreover, it exhibits excellent rate capability. Following XPS analysis of the V 2p peaks, it can be concluded that the Zn^{2+} storage mechanism of V-MOF is the reversible coordination of Zn^{2+} with the organic part, which belongs to the structurally stabilized solid solution reaction.

A summary of the four energy storage mechanisms reveals that the zinc-ion battery's energy storage mechanism is more intricate and subject to a greater number of influencing factors than the de-embedding reaction mechanism of other alkaline ion batteries.

Most of the time, an energy storage device contains several energy storage mechanisms, and the reactions are synergistic with each other, so researchers need to analyze the specific electrode materials and electrolytes to find out which kind of energy storage mechanism is dominant.

3. Cathode materials for zinc-ion batteries

The electrochemical performance of zinc-ion battery cathode materials determines the energy storage performance of the battery to a certain extent, therefore, the research on zinc-ion battery cathode materials is gradually deepening in recent years. At present, the cathode materials for aqueous zinc-ion batteries with more studies mainly include manganese-based oxides, vanadium-based oxides, Prussian blue and its analogues, and so on. The above materials and their modification studies will be introduced next.

3.1. Manganese-based oxides

Manganese-based oxides are considered to be the best choice of cathode materials for aqueous zinc-ion batteries because of their advantages of high capacity, low toxicity, easy recycling, and multivalency (Mn^{x+}, $x=0$, 2, 3, 4, and 7). In recent years, the main manganese-based oxides that have been studied more are MnO_2, Mn_2O_3, Mn_3O_4 and MnO. Among them, MnO_2 is regarded as the most promising cathode material for aqueous zinc-ion batteries by researchers because of its low toxicity, low cost, high specific capacity, high discharge platform, good compatibility with aqueous solution and moderate redox potential [23]. Fig. 4a shows that α-MnO_2, β-MnO_2, and γ-MnO_2 all have a tunneling structure, allowing for reversible insertion/detachment of Zn^{2+}. Nevertheless, aqueous zinc-ion batteries with MnO_2 as the cathode material still face many problems, such as poor real specific capacity, severe capacity degradation, and poor cycling stability during long-term operation. The following modification methods are currently the most commonly used: composite with highly conductive carbon materials; introduction of oxygen defects; defect/vacancy engineering; and addition of small amounts of Mn^{2+} to the electrolyte.

First, α-MnO_2 has a one-dimensional 2×2 large pore structure, which is favorable for the detachment of zinc ions, and the zinc ions can pass through it freely. The basic structural unit is composed of [MnO_6] octahedral double chains, and the angles of adjacent double chains in the plane are shared. Since each zinc ion can transfer two electrons, the cell of Zn/α-MnO_2 has a higher energy storage capacity than the monovalent ion battery. Moreover, its suitable tunnel size ensures the diffusion performance of zinc ions in the pores as well as the stability of the cathode material structure; therefore, α-MnO_2 has become one of the MnO_2 cathode materials with the most attention in current research. Recently, Wu *et al.* investigated the mechanism of Zn/α-MnO_2 batteries containing a slightly acidic electrolyte using characterizations by X-ray diffraction and Raman spectroscopy [37]. They revealed a reversible solid aqueous phase transition *via* manganese dissolution-deposition reaction and a solid redox mechanism *via* zinc-ion insertion. As another example, Li *et al.* studied α-MnO_2/PCSs, a cathode material composed of porous carbon nanosheets and rod-like α-MnO_2 with a large specific surface area [17]. After cycling experiments (Fig. 4b), they found that the composite electrode had a Coulombic efficiency close to 100% and performed well in terms of cycling stability even at high current densities. The cycling experiments showed a decrease in the capacity of ordinary α-MnO_2 electrodes. This suggests that α-MnO_2-based composites with higher electrical conductivity and Zn^{2+} transport efficiency have promising applications.

Additionally, β-MnO_2 is composed of [MnO_6] octahedral units arranged in a single-chain corner-sharing configuration (Fig. 4a). This result in a 1×1 tunneling structure with a smaller diameter compared to α-MnO_2 and γ-MnO_2, making it more difficult for ions to be detached and inserted. To improve the zinc storage properties of β-MnO_2, researchers have increased its conductivity by introducing oxygen defects. For instance, Zheng *et al.* prepared oxygen-rich defective β-MnO_2 (O_d) nanorods and conducted theoretical investigations into the role of O_d in the material using first-principle calculations. Their findings indicated that O_d can shift the Fermi energy level to a lower energy level, which results in an increase in the electrical conductivity of the material. Additionally, the Mn 3d and O 2p orbitals can introduce a multitude of additional states within their energy gaps, further enhancing their conductivity. Consequently, the incorporation of oxygen defects enhances the conductivity and proton adsorption strength of β-MnO_2, thereby improving its electrochemical performance [18]. In particular, the electrochemical performance of oxygen-deficient β-MnO_2 (O_d) nanorods is superior to that of pure β-MnO_2 and commercial β-MnO_2 (com). Due to the exceptional electrical conductivity of carbon materials, the composite cathode materials achieved by combining structurally stabilized β-MnO_2 with carbon materials exhibit outstanding electrical conductivity and mechanical properties. Xin *et al.* prepared β-MnO_2/3D GPE-CNT hybrids using the high-energy vibratory ball milling method [38]. The hybrid material was then used as the cathode material for an aqueous zinc-ion battery. The electrochemical performance of the battery was tested and compared to that of pure β-MnO_2 cathode material (Figs. 4c and d). After several cycles, the addition of the hybrid material containing 3D GPE-CNT improves the electrochemical and kinetic properties of pure β-MnO_2, particularly the discharge specific capacity and cycling stability.

Then, there is γ-MnO_2, which belongs to the rhombohedral crystal system, with lower crystallinity and more lattice defects, and the tunnel structure consists of soft manganite 1×1 tunnels alternating with rhombohedral manganite 1×2 tunnels irregularly [37]. It has a more complex structure, but excellent energy storage effect, therefore, it is also the focus of recent research on Zn/MnO_2 batteries. The possibility of Zn^{2+} de-embedding and electrochemically induced multiphase transition in γ-MnO_2 was first illustrated, for example, by Alfaruqi *et al.* Measurements with an *in situ* synchrotron and X-ray diffractometer revealed that the complete embedding of Zn^{2+} transformed γ-MnO_2 from a tunneling type to the coexistence of two phases of tunneling and laminar structures, as shown in Fig. 4e (green for the laminar phase, magenta for the tunneling phase, and cyan for the spinel phase) [39]. Most of these two phases were found to revert to the original γ-MnO_2 phase after several charge-discharge cycles. In addition, Wang *et al.* combined graphene with γ-MnO_2 nanorods to create a composite that possesses both the high electrical conductivity of graphene and the high ion diffusion rate of γ-MnO_2 [40]. Graphene also serves as a protective function for the structure of γ-MnO_2. Batteries composed of these composite electrodes exhibit improved stability, capacity, and cycling characteristics (Figs. 4f and g).

Not limited to MnO_2, other manganese-based oxides can also be used as zinc-ion battery cathodes. For example, Mallick *et al.* synthesized $Zn_{0.65}Ni_{0.58}Mn_{1.75}O_4$ by defect engineering of $ZnMn_2O_4$, which for the first time demonstrated the Zn^{2+} storage performance of this defect-engineered cathode and achieved ultra-long cycle stability [41]. As shown in Figs. 5a and b, this material can achieve an ultra-long charge/discharge cycle stability of 5000 cycles at 2000 mA/g without any capacity degradation. Due to the high electrostatic repulsion between Zn^{2+} in the lattice, Zn^{2+} is not suitable for diffusion in the ideal spinel structure, and in order to promote the diffusion of Zn^{2+}, a means of incorporating a large number of Mn vacancies in spinel $ZnMn_2O_4$ was adopted. Since spinel is rich in Mn vacancies, the Zn^{2+} diffusion coefficient increases, and the electrode kinetic rate increases when the elec-

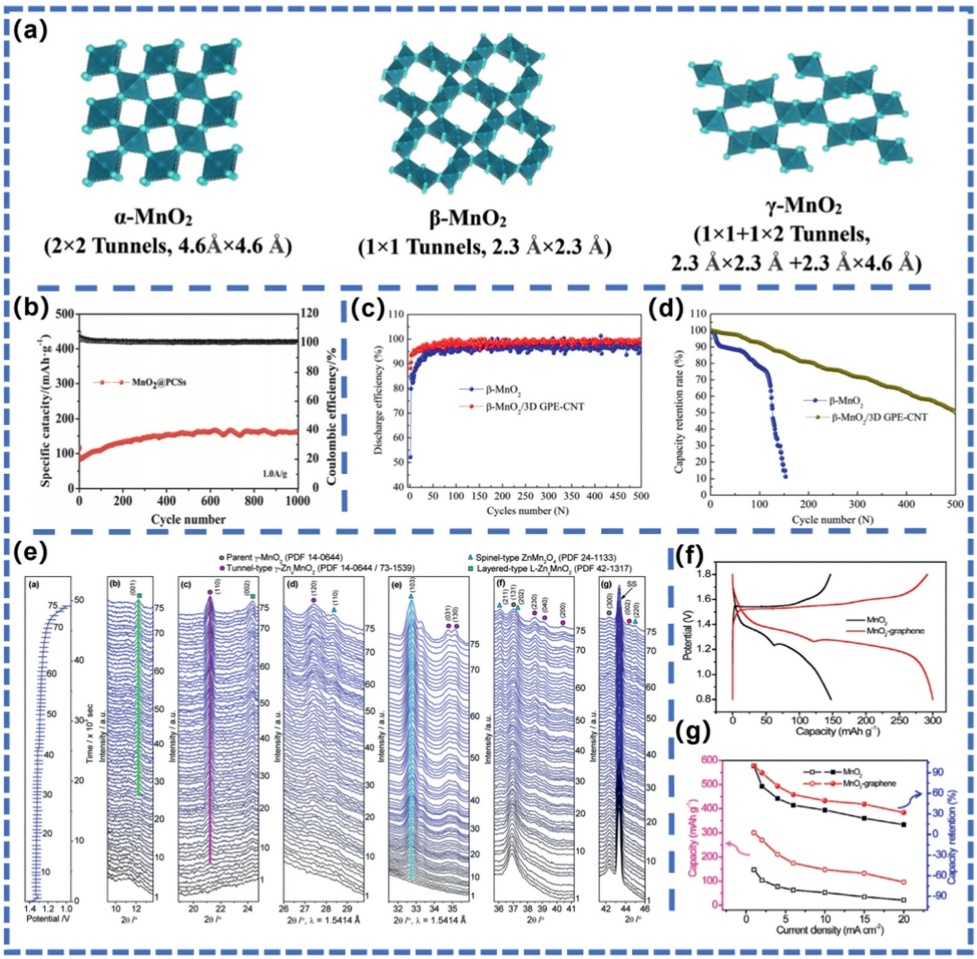

Fig. 4. (a) Schematic diagrams of the crystal structure of MnO_2 from left to right: α-MnO_2; β-MnO_2; γ-MnO_2. Reproduced with permission [37]. Copyright 2023, American Chemical Society. (b) Plot of long-cycle performance and coulombic efficiency of α-MnO_2/PCSs composites. Reproduced with permission [17]. Copyright 2021, Acta Chimica Sinica. (c) Discharge efficiency curves for pure β-MnO_2 and hybrids. (d) Capacity decay rate versus number of cycles for pure β-MnO_2 and hybrids. Reproduced with permission [38]. Copyright 2023, Elsevier. (e) Electrochemical discharge curves of the fabricated spectroelectrochemical cells cycled at a current rate of 1.4–0.8 V, 0.1 mA/cm^2, and the *in situ* XRD patterns obtained within selected scanning angle (2θ) domains of 9.2°−13.65°, 18.9°−24.8°, 26°−30°, 31.5°−35.6°, 35.7°−41.2°, and 41.3°−46°. Reproduced with permission [39]. Copyright 2015, American Chemical Society. (f) Charge-discharge curves recorded at 1 mA/cm^2 for manganese dioxide and manganese dioxide graphene electrodes. (g) Capacity and capacity retention calculated from the discharge curves of manganese dioxide and manganese dioxide graphene electrodes. Reproduced with permission [40]. Copyright 2020, Elsevier.

trostatic force against Zn^{2+} is small. Then Yin *et al.* synthesized Mn_3O_4@C as a cathode material for zinc-ion batteries, which improved the specific capacity and long-cycle performance of the batteries (Figs. 5c–e) [29].

Although manganese-based oxides have a very good electrochemical energy storage effect in zinc-ion batteries, they also face many problems, such as weak electrical conductivity. It is possible to compound manganese-based oxides and carbon materials, which not only plays a role in improving the electrical conductivity, but also provides a skeleton for manganese-based materials to prevent their dissolution or manganese-based structure destruction during charging and discharging, and enhances the charging speed and electrochemical cycling stability of the cathode materials. The electrochemical performance of β-MnO_2 hybrid material with 3D GPE-CNT added is shown in Figs. 4c and d compared with that of pure β-MnO_2 [38]; and the electrochemical performance of Mn_3O_4@C as the cathode material for zinc-ion batteries is shown in Figs. 5c–e compared with that of Mn_3O_4@C [29]. Obviously, the manganese-based oxides compounded with carbon materials have stronger chemical stability and improve the battery specific capacity and long-cycle performance. Further, the dissolution of Mn^{2+} during cycling causes a significant decrease in the specific capacity of MnO_2 materials [41,42]. Cycling test experiments on Zn/MnO_2 cells in a 2 mol/L $ZnSO_4$ electrolyte are shown in Fig. 5f by Wu *et al.* [42]. A comparison of the theoretical specific capacity calculated from the average Mn oxidation state change with the actual specific capacity determined electrochemically, where the Mn redox reaction accounts for the Faraday capacity, shows a significant decrease in the capacity of the cell. Elemental analysis of the dissolved Mn^{2+} showed that Mn^{2+} was gradually dissolved in the electrolyte, and the rate of dissolution gradually slowed down as the number of cycles increased. The reason for this situation may be that the dissolution of Mn^{2+} at the positive electrode replenishes Mn^{2+} in the electrolyte and inhibits the dissolution of Mn^{2+} instead. Therefore, the prior addition of a certain amount of Mn^{2+} can neutralize and balance the two processes of Mn^{2+} dissolution and Mn^{2+} reoxidation in the electrolyte, and thus achieve high stability of the electrode [43]. This method of adding Mn^{2+} to the electrolyte is applicable in many cases, such as adding a small amount of $MnSO_4$ or $Mn(CF_3SO_3)_2$ to $ZnSO_4$ electrolyte [42] and $Zn(CF_3SO_3)_2$ electrolyte [44], respectively.

3.2. Vanadium-based oxides

In the field of zinc-ion batteries, vanadium-based oxides are an important cathode material due to their low cost, abundant

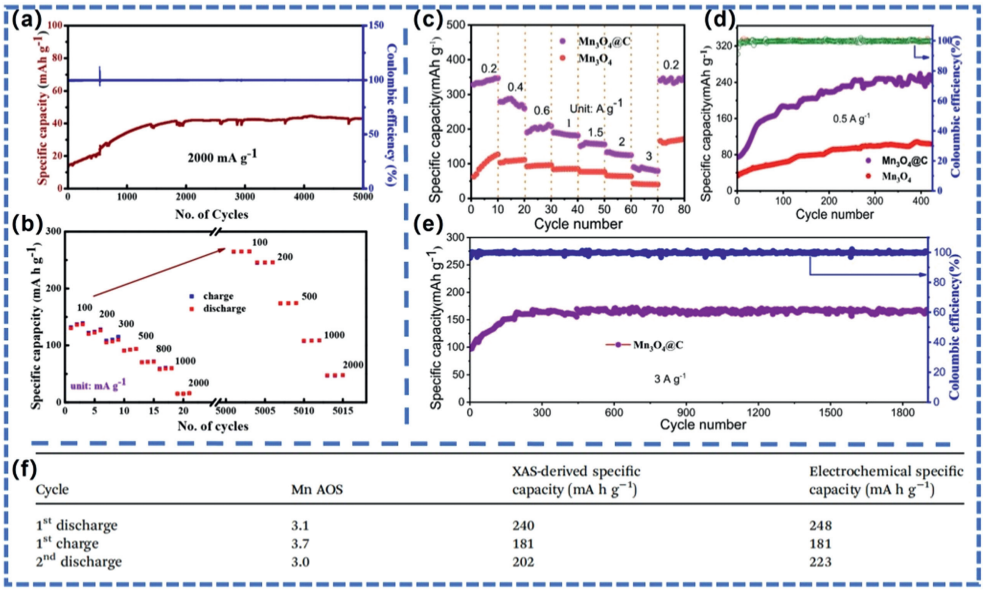

(f)

Cycle	Mn AOS	XAS-derived specific capacity (mA h g^{-1})	Electrochemical specific capacity (mA h g^{-1})
1st discharge	3.1	240	248
1st charge	3.7	181	181
2nd discharge	3.0	202	223

Fig. 5. (a) Long-term cycling performance at 2000 mA/g. (b) Rate capability before and after cycling of $Zn_{0.65}Ni_{0.58}Mn_{1.75}O_4$-based zinc-ion batteries [41]. Copyright 2022, American Chemical Society. Electrochemical performance of the Mn_3O_4@C cathode: (c) Rate characteristics, (d) cycling performance at 0.5 A/g and (e) 3 A/g [29]. Copyright 2022, American Chemical Society. (f) Comparison of the theoretical specific capacity calculated from the average manganese oxidation state change with the actual specific capacity determined electrochemically [42]. Copyright 2023, Royal Society of Chemistry.

resources, and multiple valence states for multi-step redox. This makes vanadium-based materials theoretically capable of high theoretical capacity [7]. The energy storage mechanism in zinc-ion batteries is mainly based on the intercalation and delamination of zinc ions between the lattices of vanadium-based oxides. During discharge, Zn^{2+} are inserted into the cathode while Zn in the anode loses electrons to form Zn^{2+}, thus maintaining the charge balance of the electrolyte. During reverse charging, Zn^{2+} are extracted from the cathode into the electrolyte, and Zn^{2+} in the electrolyte gain electrons (*i.e.*, are reduced) and are deposited on the Zn anode. Since vanadium-based compounds usually have different crystal structures (*e.g.*, tunneling structure of VO_2 and layered structure of V_2O_5), it gives them a variety of open structures, which facilitates the insertion and detachment of zinc ions. Vanadium-based cathode materials have higher capacities and superior cycling stability than common manganese-based compounds [45], despite having lower discharge voltages. As a result, vanadium-based oxides have become a promising cathode material for aqueous zinc-ion batteries in recent years.

First of all, VO_2 is a common cathode material in zinc-ion batteries, which is a phase transition metal oxide with a tunnel framework structure, and is available in tetragonal crystal system VO_2(A), monoclinic crystal VO_2(B), and VO_2(D) crystal types. Among them, monoclinic crystal VO_2 (B and D) has good structural stability, which provides for the reversible detachment and insertion of Zn^{2+} and is an ideal cathode material for zinc-ion batteries [46]. Moreover, the diffusion energy barriers of various materials, as calculated by DFT, can be employed to analyze the diffusion kinetics of Zn^{2+}, thereby enabling the prediction of the electrochemical performance of cathode materials. For example, Huang Juanjuan and her team at Lanzhou University constructed a VO_2@V_2C 1D/2D heterostructure (Figs. 6a and b) by controlled partial oxidation of V_2C *via* hydrothermal method [47]. This unique heterostructure improves the diffusivity of zinc ions and significantly improves the rate performance of VO_2, which achieves high capacity and maintains high multiplicity performance in aqueous zinc-ion batteries. In addition, some researchers have prepared materials with higher transport efficiency of ions by adjusting the microscopic morphology of monoclinic crystalline VO_2(D), which has a larger specific surface area, a larger layer spacing or a core-shell structure. For example, Chen *et al.* prepared monoclinic crystalline VO_2(D) with nanosphere hollow structure [48]. This hollow internal structure made the diffusion of Zn^{2+} into the interior of the electrode material easier, and the multiplicity performance and cycle life of the electrode remained good under the condition of large loading area. In general, the discharge specific capacity and cycle stability of the battery were improved.

In the second place, V_2O_5 is also a common cathode material, which belongs to the rhombohedral crystal system and is a typical layered vanadium-based oxide. The distance between the layers of V_2O_5 is larger than the radius of Zn^{2+}, and ions are free to de-embed between the layers during the charging and discharging process [45]. The electrostatic interaction present in the crystal structure of V_2O_5 hinders the detachment of Zn^{2+}, and with repeated detachment of ions, the van der Waals forces between the laminar structures are gradually weakened, and the reversibility and kinetic properties of the Zn^{2+} detachment process are affected by the number of detachments and the number of cycles. As mentioned previously, compounding with highly conductive carbon materials improves the conductivity of the materials, and similarly, excellent conductivity can be obtained by compounding V_2O_5 with carbon materials. Muthukumar *et al.* used a microwave-assisted process of liquid-phase exfoliation to produce vanadium pentoxide nanoribbons (NRs) [49]. These NRs were then assembled with graphene oxide (GO) nanosheets to create highly conductive V_2O_5 NR/GO hybrids (Fig. 6c). Zhang *et al.* synthesized V_2O_5 (V_2O_5@PPy) nanospheres with oxygen vacancies coated with PPy, which exhibited a high capacity (404.3 mAh/g at 0.2 A/g), enhanced transport properties, and excellent cycling stability (268.1 mAh/g after 1000 cycles), as shown in Figs. 6d and e [50]. Meanwhile, in order to improve the electrode kinetic performance and accelerate the de-embedding of Zn^{2+}, some researchers inserted structured water molecules into V_2O_5 to obtain $V_2O_5{\cdot}nH_2O$ with a bilayer structure. Compared to the raw material, this bilayer structure has a larger layer spacing that facilitates the de-embedding of Zn^{2+}. The inserted water molecules attenuate the interlayer elec-

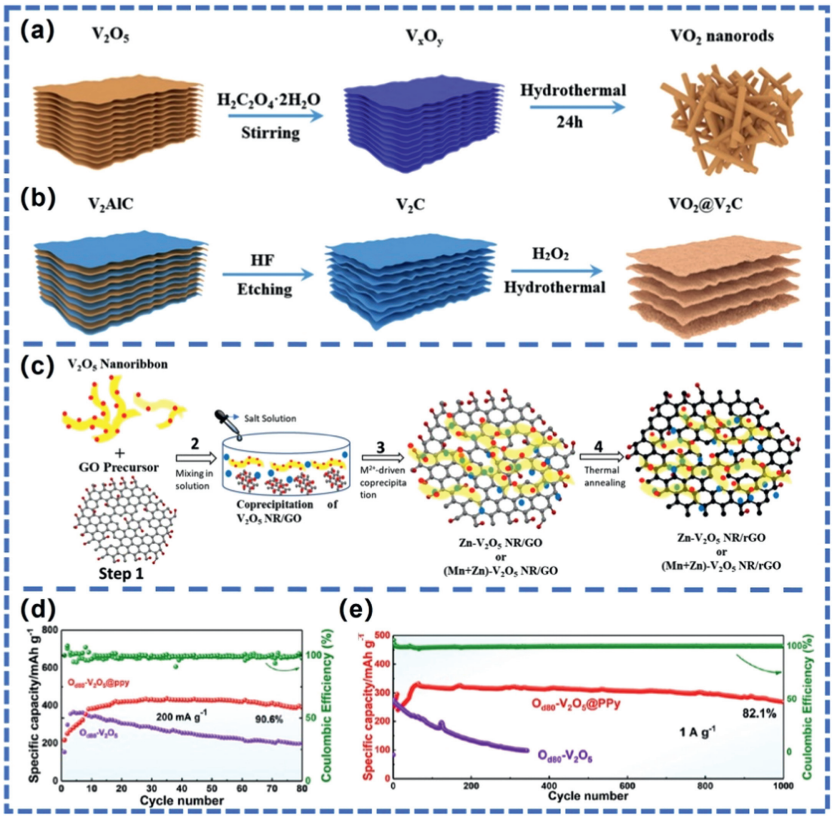

Fig. 6. (a) Schematic diagram of the preparation process of vanadium dioxide nanorods. (b) Schematic diagram of the synthesis of $VO_2@V_2C$ 1D/2D heterostructures. Reproduced with permission [47]. Copyright 2022, American Chemical Society. (c) Schematic diagram of co-precipitation synthesis of V_2O_5 NR/rGO hybrids. Reproduced with permission [49]. Copyright 2023, American Chemical Society. (d) Cycling performance of O_{d80}-V_2O_5 and O_{d80}-V_2O_5 at 200 mA/g. (e) Long-term cycling performance of O_{d80}-V_2O_5 and O_{d80}-V_2O_5@PPy at 1 A/g. Reproduced with permission [50]. Copyright 2023, American Chemical Society.

trostatic force caused by the excessively high positive charge of Zn^{2+}, which is conducive to the diffusion and transfer of ions. This optimization improves the multiplicity and electrochemical performance of the battery system [49,51].

In addition to the more common vanadium-based oxides, vanadium-based compounds represent a significant area of research interest in the field of cathode materials for aqueous zinc ion batteries. For instance, Ren *et al.* proposed a novel porous $K_{0.5}VOPO_4{\cdot}1.5H_2O$ polyanion cathode (P-KVP) for the first time, which is not only capable of achieving high output voltages (>1.2 V), but also can be mass-produced by using a simple technology [15]. Furthermore, Wu and his research team prepared PEO-LiV_3O_8 superlattice nanosheets with an extended interlayer spacing (1.16 nm) in order to address the issue of slow transport kinetics of Zn^{2+} in the cathode lattice and to enhance the mass loading performance [52]. The experimental results are in agreement with density-functional theory simulations, which indicate that the interlayer PEO helps to reduce the Zn^{2+} diffusion resistance and increase the number of active sites at additional interfaces, thus improving the Zn^{2+} storage rate.

In conclusion, vanadium-based compounds with multiple oxidation states, abundant crystal structures and natural reserves are considered as the most prospective cathode materials for zinc-ion batteries. Vanadium-based cathode materials can be used in zinc-ion batteries by modulating local electroneutrality and lowering the diffusion ion barrier. This allows electrolyte cations to nest within the electrode material, providing greater practical capacity [1,15,28,49]. The following modifications are common in current research on vanadium-based oxides: bonding with highly conductive carbon materials; embedding structural water molecules; and modulating localized electroneutrality and lowering diffuse ionic barriers.

3.3. Prussian blue analogues

Prussian blue analogs (PBAs) are transition metal hexacyanoferrates, such as nickel hexacyanoferrate (NiHCF), copper hexacyanoferrate (CuHCF), and zinc hexacyanoferrate (ZnHCF), with a 3D network structure. They have become a research hotspot in zinc-ion batteries because their open framework structure allows for the highly reversible insertion/extraction of zinc ions (Fig. 3e) [35].

The structure of PBAs has a large gap, which favors the de-embedding of Zn^{2+}. The de-embedding of ions is also influenced by water molecules and alkali metal atoms. So far, by applying Ni-HCF and FeHCF, CuHCF and ZnHCF to zinc-ion batteries, it has been found that all of them have the potential to be used as cathode materials, with NiHCF and FeHCF having a typical cubic structure, and ZnHCF having a rhombic skeletal structure. For example, the Zn||CuHCF hybrid cell fabricated by Li *et al.* in NZDES-2 electrolyte is shown in Figs. 7a and b showing a good stability of 91.6% after cycling for 3000 cycles at a rate of 10 C [53]. Xu *et al.* investigated the cathode material of zinc hexacyanoferrate (ZnHCF) in aqueous zinc-ion batteries [19]. They found that the morphology of the cathode material was affected by the concentration of the precursor solution and the valence state of the iron ions. The rhombic ZnHCF structure had a high degree of crystallinity, with diameters ranging from 700 nm to 2 μm (Figs. 7c and d). Additionally, the Zn-HCF exhibited a large capacity of 66.7 mAh/g. Yang *et al.* explored an aqueous zinc-ion battery with $FeFe(CN)_6$ as the positive electrode and a Zn-Na hybrid electrolyte, and found that the discharge

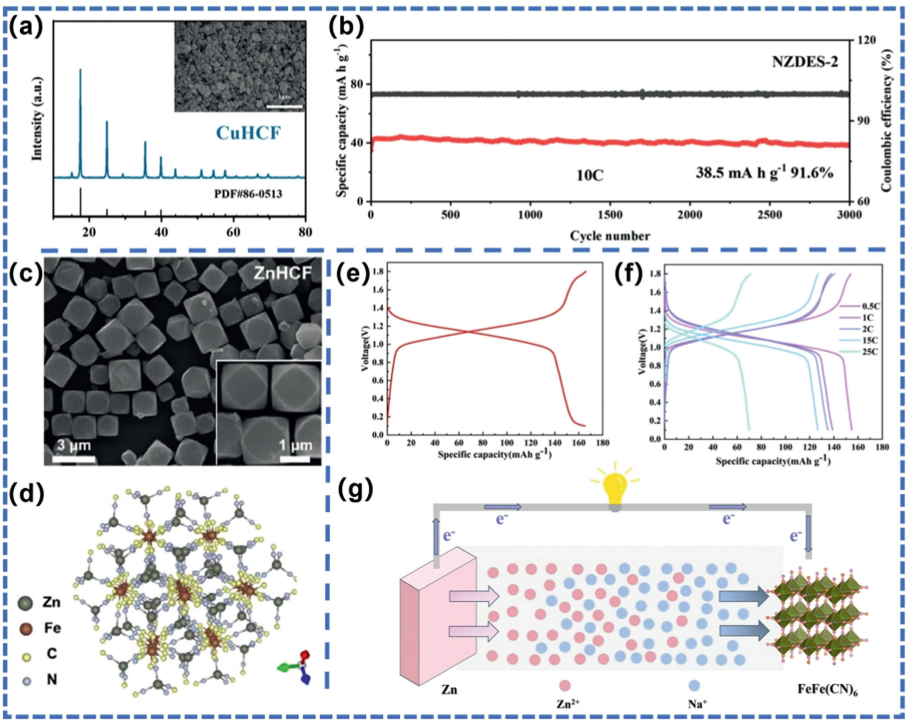

Fig. 7. (a) XRD image of CuHCF material. (b) Cycling performance of Zn||CuHCF hybrid cell at a rate of 10 C [53]. Copyright 2023, American Chemical Society. (c) Schematic of scanning electron microscope (SEM) image of ZnHCF. (d) Localized structure of ZnHCF [54]. Copyright 2022, American Chemical Society. (e) First discharge-charge curves at 0.1 C (0.1–1.8 V). (f) Charge-discharge curves at different current densities from 0.5, 1, 2, 15 and 25 C. (g) Schematic diagram of the Zn//$FeFe(CN)_6$ rechargeable aqueous hybrid cell [55]. Copyright 2023, Royal Society of Chemistry.

capacity of this battery was as high as 165.2 mAh/g at 0.1 C, which is superior to many reported aqueous zinc-ion batteries or Zn-Na hybrid batteries (Figs. 7e–g) [54]. Xiang *et al.* assembled and tested an aqueous zinc-ion battery with NiHCF as the cathode material, and systematically investigated the effect of different Zn^{2+} coordination configurations on the reversibility of the zinc anode in the Zn/NiHCF full cell [55].

In conclusion, compared with inorganic materials, PBAs have the following advantages: (1) High voltage and stable crystal structure [53]; (2) Large and unique three-dimensional ion channels, which are suitable for rapid insertion and detachment of Zn^{2+} [54]; (3) It can provide more active sites [12,19]. However, their low practical capacity limits the development of the whole system and makes them uncompetitive for zinc-ion battery cathode material applications. In addition, the structural evolution and valence changes of transition metal atoms in PBAs are complex and remain to be further investigated in depth.

4. Zinc anode materials for zinc-ion batteries

In aqueous zinc-ion batteries, zinc metal is commonly used as the negative electrode due to its stability and high theoretical specific capacity of 820 mAh/g (5855 mAh/cm^3) [14,28]. Zinc is a transition metal with an atomic number of 30. It has a silver-gray appearance and high electrical conductivity. Zinc is amphoteric, meaning it can react with both acids and bases. When reacting with acid, it generates Zn^{2+}, and when reacting with alkali, it generates $[Zn(OH)_4]^{2-}$.

4.1. Advantages of zinc metal

(1) Abundant reserves. Zinc is the fourth most common metal and has abundant reserves in the earth's crust. China has particularly abundant zinc ore resources, with zinc reserves ranking fourth in the world.

(2) Non-toxic and environmentally friendly. As an essential trace element, metallic zinc and zinc ions are virtually harmless to the human body. Zinc and zinc-containing compounds are also relatively friendly to the atmosphere and soil [56]. This suggests that aqueous zinc-ion batteries, based on zinc metal negative electrodes and zinc ion electrolyte-based zinc ion batteries, can be used in a wider range of applications.

(3) Low cost. Compared to secondary batteries that use alkali metal negative electrodes, which are more commonly studied in organic systems, batteries that use zinc metal are more economical due to the lower cost of zinc compared to Li/Na/K metals, aluminum, and copper collectors, which are the most commonly used materials in secondary batteries [2].

(4) High theoretical capacity. Ultra-high theoretical capacity of 820 mAh/g (5855 mAh/cm^3) can be realized by using zinc metal directly as electrode [14].

(5) Low redox potential. Regarding the standard hydrogen electrode, zinc metal has a low redox potential of −0.76 V. This potential is higher than the overpotential of water decomposition by hydrogen precipitation on the surface of zinc. This implies that zinc metal can be stabilized and reversibly redoxed in an aqueous electrolyte [57]. Zinc is the most promising anode material for aqueous batteries, as shown in Fig. 8a.

4.2. Existing issues

Zinc-ion batteries face several issues with their negative electrodes, including zinc dendrite, passivation, and self-hydrogen precipitation. The problems of dendrite and passivation are caused by the non-uniform Zn^{2+} dissolution/deposition reaction on the zinc negative electrode, which can harm battery performance.

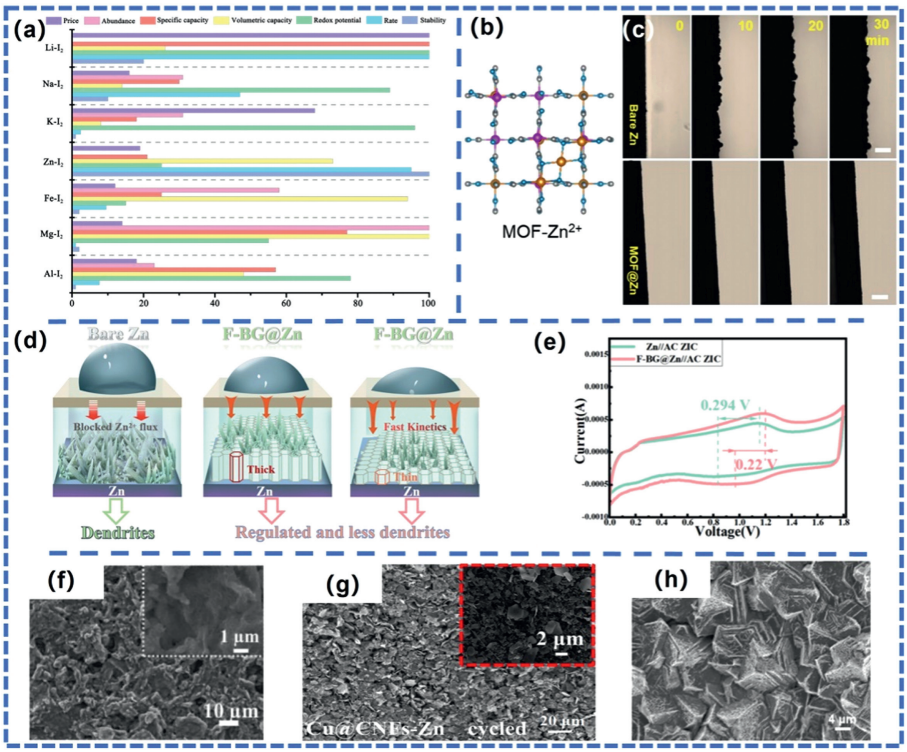

Fig. 8. (a) Schematic visualization comparing different metal iodide cells in terms of price, abundance, specific capacity, volumetric capacity, redox potential, rarity, and stability. Reproduced with permission [14]. Copyright 2023, Royal Society of Chemistry. (b) Top-view structural model of zinc atoms on MOF substrate. (c) *In situ* optical micrographs of zinc deposition on bare Zn and MOF@Zn at a current density of 5 mA/cm^2 (scale bar: 50 μm). Reproduced with permission [58]. Copyright 2023, American Chemical Society. (d) Schematic of the mechanism of Zn dendrite inhibition by F-BG@Zn. (e) CV curves of Zn//AC and F-BG@Zn//AC hybrid capacitors at a scan rate of 2 mV/s. Reproduced with permission [59]. Copyright 2023, American Chemical Society. (f) FESEM image of TiO_2-CNT@Zn anode. Reproduced with permission [8]. Copyright 2023, Elsevier. (g) SEM image of Cu@CNFs-Zn after 50 cycles at 1.0 mA/cm^2. Reproduced with permission [3]. Copyright 2022, American Chemical Society. (h) FESEM image of Zn@NOG. Reproduced with permission [60]. Copyright 2023, American Chemical Society.

(1) During the battery's operation, the anode's metal zinc undergoes constant oxidation, producing zinc ions that are then reduced back into metal zinc. This reduction process often results in the deposition of metal zinc in the same location as before, causing the formation of zinc dendrites to increase with each charge/discharge cycle. If the zinc dendrites grow enough to penetrate the diaphragm, they can short-circuit the battery by coming into contact with the positive electrode. This poses a safety hazard when using the battery. Additionally, dendrites generated at the tendency position are randomly distributed and cause electrode deformation, leading to battery capacity degradation [57].

(2) Passivation of the zinc electrode occurs primarily in alkaline electrolytes. Zn^{2+} reacts with OH^- to produce insoluble ZnO or $Zn(OH)_2$, which forms a passivation film on the electrode surface. This film isolates the contact between zinc and the electrolyte, reducing the reactive surface area of the zinc electrode. As a result, the dissolution of metallic zinc is hindered, and the sustained discharging state of the battery is affected, which reduces the activity and cycling performance of the battery [11].

(3) To ensure proper battery operation, an excess of zinc must be supplied due to the continuous consumption of zinc metal through the hydrogen precipitation process. In sealed batteries, corrosion causes hydrogen to precipitate, increasing pressure within the battery case. If the pressure exceeds the limit, the battery may expand and rupture, leading to electrolyte leakage [12]. During operation, hydrogen precipitation reactions increase the local concentration of hydroxides and form insoluble substances, which are an important source of hydroxides.

During battery charging and discharging, dendrites, hydrogen precipitation reaction, and electrochemical corrosion can interact with each other [7,14]. The formation of dendrites increases the negative electrode's surface area, accelerating the rate of hydrogen precipitation and generating more OH^-. This, in turn, accelerates the electrode's passivation and makes the surface more prone to dendrite formation, leading to more severe electrode polarization and easier dendrite formation.

4.3. Modification methods

To tackle the aforementioned issues, three primary design strategies are employed: modifying the structure of the zinc electrode, optimizing additives, and developing zinc alloying. The design strategies are based on the principles of ensuring uniform charge distribution over the anode surface, stabilizing zinc deposition/stripping, and limiting side reactions. The following sections will describe each of these strategies in detail.

4.3.1. Modifying the structure of the zinc electrode

The formation and corrosion of zinc dendrites are mainly caused by the uneven distribution of Zn^{2+} on planar or two-dimensional metallic zinc foils.

(1) To improve the uniformity of Zn^{2+} deposition and reduce the formation of zinc dendrites and corrosion problems, the method of changing the structure of the zinc electrode can be adopted. This includes constructing an anode with a large electroactive surface area and high conductivity, using a zinc electrode with a porous structure or a collector with a layered structure, and increasing the surface area of the zinc

anode so that the area involved in the reaction increases, which is conducive to the uniformity of the deposition of Zn^{2+}. Similarly, optimizing electrode performance can be achieved by using layered collectors with high electroactive surface area and uniform electric field, which change the structure of the zinc electrode.

Zinc can be electrodeposited on highly conductive, porous, nano or microstructured substrates, such as metal-organic frameworks (MOFs). MOFs have three-dimensional open frameworks, adjustable compositions, and controllable pore structures, which effectively homogenize the Zn^{2+} fluxes. This ultimately leads to fast and stable zinc plating kinetics and dendrite-free zinc anodes (Fig. 8b). Sun *et al.* constructed a 7 μm thick MOF interfacial layer that effectively inhibits side reactions and self-corrosion (Fig. 8c) [58]. Additionally, the MOF layer improves zinc deposition kinetics and inhibits zinc dendrites, resulting in a stable polarization voltage for MOF@Zn. In contrast, planar Zn foils serve as both active materials and collectors. However, their mass, volume, and electrical properties may change with the deposition/exfoliation of Zn, which can lead to unstable cycling performance.

Deposition of zinc into layered collectors is a viable method for slowing down dendrite growth and achieving high rate and stable ZIBs. Wang *et al.* designed a sulfonated functionalized boron nitride/graphene oxide (F-BG) buffer layer, a unique nanosheet that directs a uniform zinc flux and efficiently achieves homogeneous nucleation on zinc foils through a homogeneous interfacial electron field, as shown in Fig. 8d, thereby mitigating dendrite growth and HER side reactions [59]. The anodes obtained through this method exhibit higher capacity and smaller polarization in comparison to conventional zinc foils (Fig. 8e). Additionally, the zinc nano-array structures demonstrate excellent electrochemical activity and fast Zn/Zn^{2+} redox kinetics. Moreover, many similar studies have been conducted for this technology, such as the zinc-coated TiO_2-CNT anode shown in Fig. 8f [8], the zinc-coated Cu@CNT anode shown in Fig. 8g [3], the zinc-coated three-dimensional nitrogen-oxygen co-doped graphene anode shown in Fig. 8h [60], and the zinc-coated nickel-titanium alloy yarns. This new type of zinc hierarchical current-collecting anode greatly reduces the formation of dendrites, which is conducive to improving multiplicity performance and lifetime.

(2) Introducing a protective layer on the zinc surface is also a structural design method. Functional materials such as carbon-based materials, inorganic non-metallic materials, and polymeric materials have been found to serve as protective layers for zinc deposition. To homogeneously strip/plate the zinc and inhibit hydrogen evolution and surface corrosion, it is possible to protect the zinc from direct contact with the electrolyte, for example, by using ultrathin titanium dioxide, or by limiting the nucleation sites of the zinc, for example, by using nanoporous calcium carbonate.

Carbon-based materials have good electrical conductivity and can be used to stabilize the de-embedding behavior of Zn^{2+} by changing the zinc anode interface. For example, Zhang *et al.* prepared zinc metal with an ultrathin carbon coating (C@Zn) by magnetron sputtering, which increased surface wettability, resulted in a more homogeneous zinc coating, and mitigated undesirable side effects [61]. Kim *et al.* used plasma treatment for surface engineering to enhance the oxygen functionalization of graphene layers [62]. The surface-functionalized graphene layer effectively prevented the proliferation of zinc dendrites and stabilized the interface between the anode and electrolyte. The obtained ZIBs exhibited superior storage performance and reversibility, with a specific capacity of 260.0 mAh/g at 0.3 A/g and a long-term stability of 150 cycles at 2.0 A/g and a specific capacity of 139.0 mAh/g. Later, Zheng *et al.* prepared porous biomass carbon material (BCK) with larger specific surface area and used BCK as an interfacial coating for zinc anode [9]. As shown in Figs. 9a–c, it was experimentally demonstrated that BCK-7 has abundant pore structure and zinc-friendly oxygen-containing functional groups, which can provide more active sites for Zn^{2+} nucleation and help to better mitigate the occurrence of zinc dendrites and side reactions, and to improve the cycle life and cycle stability of the battery. The full-cell battery consisting of BCK-7@Zn anode and MnO_2 cathode remained 61.5% after 1000 cycles (Fig. 9d). The incorporation of these carbon-based materials improves the cycling stability and electrochemical performance of zinc anodes by modulating the growth of zinc dendrites or dendrites.

In addition to carbon-based materials, inorganic non-metallic materials that do not react with the zinc anode are also suitable for use as a protective layer for the zinc anode, such as titanium dioxide TiO_2, calcium carbonate $CaCO_3$, and zirconium dioxide ZrO_2. Liang *et al.* obtained electrodeposited manganese dioxide (EMD) on zinc substrate by electrodeposition under constant pressure conditions, and the protective layer can extend the lifetime of the battery by improving its corrosion resistance [63]. As another example, Li *et al.* modified a zinc anode with a nanoporous coating composed of niobium pentoxide (Nb_2O_5) for uniform zinc deposition [64]. Compared with the bare zinc anode, the surface of Nb_2O_5@Zn anode was smoother and more uniform, and the zinc flakes were deposited on the surface in parallel and uniformly, and the Nb_2O_5 coating could effectively guide the uniform deposition of zinc (Figs. 9e and f). Therefore, the zinc anode modified by Nb_2O_5 coating can realize better cycle stability and rate capability. In addition, Yu *et al.* constructed a strong protective layer of sodium zinc phosphate (Zn@NZP) *in situ* on the zinc metal foil anode, and the schematic diagram of the preparation process and the mechanism of inhibition of dendrites in the electrolyte are shown in Fig. 9g [65]. This NZP coating inhibits the formation of dendrites and side reactions, and reduces the energy barriers for zinc ion electroplating and stripping.

Polymeric materials can also be used as protective coatings for zinc anodes to improve interfacial properties. Recently, researchers have developed a new three-dimensional porous zinc anode (PF@Zn) to prevent the disordered growth of dendrites and by-products [66]. The corrosion potential of the PF@Zn electrode (−0.968 V) was higher than that of the bare Zn electrode (−0.979 V), and the corrosion current density (−1.83 mA/cm^2) was lower than that of the Zn electrode (−1.52 mA/cm^2), which suggests that the corrosion performance of the PF@Zn electrode is dominant. The PF@Zn electrodes have a high CE value (99.1%) and an extremely long service life (240 h) at a relatively high plating capacity of 1 mAh/cm^2 due to the three-dimensionally interconnected porous substrate that improves the anode's corrosion resistance and uniformly strips Zn^{2+}. Furthermore, the C//PF@Zn capacitors maintain a high capacity of 96.6% even after 3000 cycles at 1.5 A/g.

4.3.2. Optimizing additives

Additive materials can be classified into two categories: (1) Structural modifiers, which optimize the anode structure (*e.g.*, three-dimensional porous structure) to suit the anode product formed; (2) Morphological modifiers, which adjust the surface morphology or crystal orientation to prevent dendrite growth on specific crystal faces.

(1) Activated carbon (AC) can be used as a structure modifier for Zn anodes due to its high porosity structure. During the charging process, Zn deposition is more likely to occur inside the pores of the AC than on the surface (Fig. 10a). This results in the absorption of formed Zn dendrites

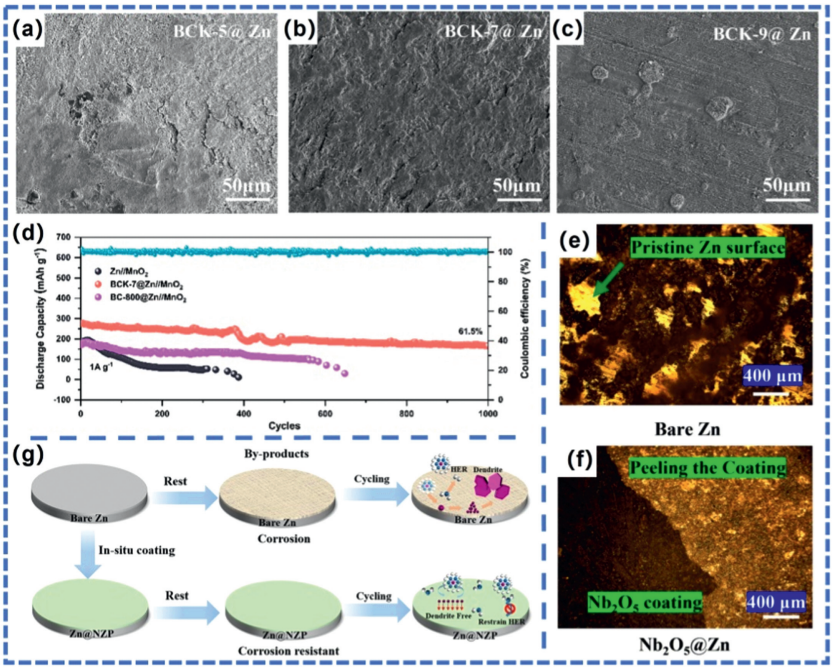

Fig. 9. SEM images of symmetric cells of (a) BCK-5@Zn, (b) BCK-7@Zn, and (c) BCK-9@Zn after 100 h of cycling. (d) Cycling performance of the different cells and the Coulombic efficiency of the BCK-7@Zn//MnO_2 cell [9]. Copyright 2024, Elsevier. Optical images of the surface of the Zn anode after 50 cycles for (e) bare Zn anode and (f) Nb_2O_5@Zn anode [64]. Copyright 2024, Elsevier. (g) Schematic of the preparation process of Zn@NZP anode and the mechanism of dendrite inhibition in the electrolyte [65]. Copyright 2023, American Chemical Society.

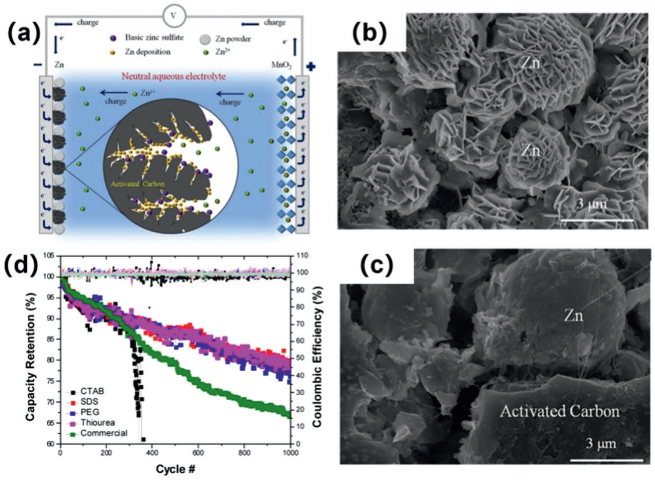

Fig. 10. (a) Schematic diagram of zinc deposition in activated carbon during charging. (b) Scanning electron microscope image of unmodified zinc anode after 80 cycles. (c) Scanning electron microscope image of AC-modified zinc anode after 80 cycles. Reproduced with permission [67]. Copyright 2015, The Electrochemical Society. (d) Cycling stability of cells using commercial zinc foil anodes and electroplated zinc anodes with different organic additives. Reproduced with permission [6]. Copyright 2017, American Chemical Society.

and anode by-products (alkaline Zn sulfate) into the well-developed pores, leaving a smooth Zn anode surface (Figs. 10b and c). The cycling reversibility of the battery with AC-modified Zn anode was effectively enhanced, resulting in a capacity retention rate of 85.6% after 80 cycles. This is a significant improvement compared to the unmodified Zn anode, which only retained 56.7% of its capacity [67].

(2) Several studies have been conducted on the inhibition of dendrites by various organic additives in neutral and acidic mild electrolytes. These include sodium dodecyl sulfate (SDS), cetyltrimethylammonium bromide (CTAB), polyethylene glycol (PEG-8000), and thiourea (TU), as morphology modifiers. The formation of dendrites is affected by the weave and crystals on the surface of the zinc anode. Electroplated zinc anodes with and without organic additives display different crystal orientations due to changes in surface energy induced by the organic additives. Table 1 shows that Zn-PEG has a strong crystal orientation at (103) and a crystal growth close to horizontal, indicating that Zn-PEG has the lowest probability of forming dendrites, while the dominant peaks of Zn-SDS, Zn-TU and electroplated Zn without additives are from (101) plane, which is the same as that of the dominant peaks of Zn foils. Due to the fact that crystal growth on the (101) plane is approximately 70° perpendicular to the electrode surface, dendrite formation is likely to occur on the anode of the (101) plane, which plays a dominant role. However, the addition of SDS and TU reduces the likelihood and extent of dendrite formation. This is due to the significant enhancement of other peaks, such as the (002), (102), and (103) peaks of Zn-SDS.

As shown in Fig. 10d, except for the Zn-CTAB anode, the cycling performance of the modified zinc anodes was improved compared to the commercial zinc foil anodes. This finding is consistent with the XRD results of Zn-CTAB, which indicate a stronger (101) plane. Briefly, all three organic materials, SDS, PEG, and TU, except CTAB, are effective surface modifiers that inhibit the formation of dendrites and corrosion rate on the zinc anode, thereby improving the cycling stability of the battery (Table 1). Among the three, SDS was found to be the most effective organic additive. Additionally, zinc anodes with dominant crystal orientations of (101) and (100) were found to be more prone to dendrite formation, while those with dominant planes of (002) and (103) were less likely to form dendrites.

However, this finding differs from some previous studies that have shown that electrodeposited zinc anodes without organic additives have a stronger (002) weave. The introduction of additives changes the preferred orientation from the basal plane (002) to

Table 1
Comparison of crystal properties, corrosion rates and electrochemical properties of electroplated zinc and commercial zinc foils with and without additives.

Zinc anode	Dominant peak	Corrosion potential (mV)	Corrosion current ($\mu A/cm^2$)	Average capacity retention after 100 cycles (%)
Commercial zinc	(101) (103)	0 ± 2	1422 ± 110	67
Additive free zinc	(101) (103) (002)	4 ± 5	1136 ± 82	–
Zn-CTAB	(101) (100) (103)	2 ± 2	220 ± 7	12
Zn-SDS	(101) (103) (102)	2 ± 5	75 ± 14	79
Zn-PEG	(103) (102) (002)	11 ± 8	163 ± 32	76
Zn-Thiourea	(101) (102) (103)	10 ± 8	43 ± 7	80

(100) and (110). The studies share a common finding that the crystal orientation of electrodeposited Zn is altered by surface modifiers. This is because organic surfactants obstruct certain active sites and interact electrostatically with Zn^{2+}, leading to distinct growth kinetics during zinc electrodeposition. Future studies should explore the effects of inorganic additives on the surface morphology and crystal structure of electroplated zinc anodes. It is important to note that this strategy may not be suitable for large-scale applications due to the toxicity and high cost of most additives.

In conclusion, the synthesis of electroplated zinc anodes using auxiliary substrates and additives is an effective strategy to inhibit dendrite growth and improve recharging capacity. This may be due to the purification of zinc during electrodeposition or electroplating, as impurities in commercial zinc foils can lead to uneven nucleation sites for zinc electrodeposition. Another major idea for modified zinc anodes is to increase the active surface area to increase the number of active sites for fast and homogeneous zinc plating/stripping. However, due to the complexity and high cost of existing methods, there is still a great need for reliable and easy to implement strategies. To overcome the formation of zinc dendrites, an alternative intercalation anode for ZIBs can be found, similar to the approach taken with graphite in LIBs. However, this scheme can affect the operating voltage of ZIBs. For instance, a complete ZIBs can be formed by assembling 9,10-anthraquinone (AQ) as an anode with a $ZnMn_2O_4$ cathode [68]. Though a dendrite-free anode was obtained after cycling, the high discharge potential of AQ reduced the operating voltage of the cell. Therefore, developing high-energy ZIBs by exploring zinc-free anodes may not be the best option if a high-potential cathode cannot be found.

4.3.3. Developing zinc alloying

To address issues such as dendrite growth, hydrogen precipitation, and corrosion, zinc can be alloyed with other metals. Yuan *et al.* mitigated zinc dendrite growth by alloying the anodes with rare earth elements [69]. The addition of Ce, Yb, and Mg to pure zinc anodes reduced point and surface defects, refined grain size, and decreased the anode's IEA strength, inhibiting dendrite growth. The formation of a Zn-Ni alloy film and solid-electrolyte interface (SEI) layer influences the nucleation and growth of Zn. This nickel-salt Zn coating can maintain a good state of non-porosity, resulting in excellent electrochemical performance and stability during cycling. Xie *et al.* used a copper-zinc alloy ($Cu@Cu_3Zn$) that was synthesized through a high-temperature gas-solidification reaction of zinc vapors with copper nanowires [70]. They then constructed a three-dimensional alloy network using a vacuum filtration method. The alloy network stabilized the zinc deposition interface by inhibiting two-dimensional diffusion and corrosion reactions. Additionally, it enhanced the zinc plating/stripping kinetics by accelerating the zinc desolvation and nucleation processes. Furthermore, a ZIB without an anode was created by utilizing a cathode made of $Zn_3V_3O_8$ and a collector made of copper carbide foil (CCF) modified with an alloy network. This ZIB exhibited exceptional cycling stability.

Qi *et al.* proposed a zinc-aluminum alloy that sacrificially oxidizes aluminum when immersed in an electrolyte, forming an electrochemically inactive Al_2O_3 phase on the surface of the zinc-aluminum foil. The introduction of Al_2O_3 not only directs the electrodeposition of zinc at the available zinc sites, but also reduces the oxygen content in the electrolyte and the potential for zinc passivation. Thus, zinc-aluminum alloys possess several advantages such as low corrosion rate, low dendrite formation, low corrosion current, and high capacity. These properties make them ideal for use as ZIB anodes with high speed performance and ruggedness [71].

In summary, it is evident that the design of the zinc negative electrode can be improved through structural modifications, coatings, and electrolytes to mitigate issues such as zinc dendrites, passivation, and self-precipitation of hydrogen. However, despite these efforts, the practical application of these methods still falls short, and further research is needed to identify more effective solutions.

5. Current state of research on zinc-ion battery electrolytes and their effect on the cathode interface

Electrolyte is an essential component of a battery, serving as the medium for connecting the positive and negative electrodes and facilitating ion transfer. The ideal electrolyte for aqueous zinc-ion batteries should also fulfill the following requirements: (1) A wide electrochemical window; (2) better compatibility with other components in the battery; (3) environmentally friendly and low toxicity; (4) lower cost. So far, the main electrolytes used in aqueous zinc-ion batteries are aqueous $ZnSO_4$ and zinc salts such as $Zn(CF_3SO_3)_2$. From an electrolyte standpoint, the presence of excessive free water can restrict the operating voltage range of zinc-ion batteries and result in negative electrode dendrite formation, passivation, and positive electrode dissolution. Additionally, conventional aqueous electrolytes suffer from issues such as high-temperature evaporation, intensified hydrogen precipitation, low-temperature icing, and a sharp decrease in kinetics, which severely limit the applicable environment of aqueous zinc-based batteries [32,44,68-71]. For instance, Jun Chen and their team from Nankai University disrupted the hydrogen bonding network in the $ZnCl_2$ solution by altering the concentration of $ZnCl_2$ [72]. The modulation of the electrolyte structure, including hydrogen bonding and ionic interactions, is illustrated in Fig. 11a. At 0 °C, the pristine water network connected by hydrogen bonds readily transforms into an ice network. With the addition of $ZnCl_2$, the hydrogen-bonded network undergoes a transformation. The network is disrupted due to the strong interactions between the ions and the water, while the interactions between the ions are reinforced. The $ZnCl_2$ inhibits water solidification and reduces the solid-liquid transition of the aqueous electrolyte temperature from 0 °C to −114 °C. In addition, electrode/electrolyte interface properties have been extensively studied in the field of ion batteries, particularly for solid-state electrolyte interfaces. A well-formed SEI film can effectively inhibit further reactions between the electrode and electrolyte, preventing the generation of dendrites and electrode corrosion

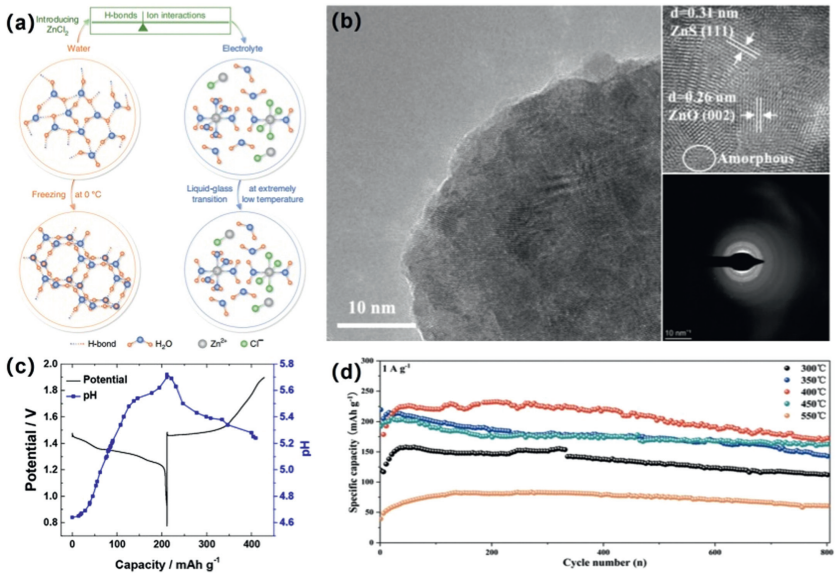

Fig. 11. (a) Schematic illustration of the structural evolution of water and electrolytes, and the design of low-Pt solutions. Reproduced with permission [72]. Copyright 2020, Nature. (b) TEM, HR-TEM and SAED images of SEI formed in $ZnSO_4$/FA electrolyte. Reproduced with permission [74]. Copyright 2024, Royal Society of Chemistry. (c) Change in pH during the first discharge-charge process. Reproduced with permission [30]. Copyright 2016, Chemistry Europe. (d) Comparison of long-term cycling of MnOOH nanorods obtained after thermal treatment at different temperatures at a current density of 1 A/g. Reproduced with permission [18]. Copyright 2023, Royal Society of Chemistry.

[11,14,53,59]. Due to the specificity of SEI membranes, it is widely accepted that they can only be formed in non-aqueous electrolytes. It is also challenging to form stable SEI membranes in aqueous energy storage systems [73]. Li *et al.* recently proposed using organic small molecule formamide (FA) as an additive to aqueous $ZnSO_4$ electrolyte to form an inorganic-organic bilayer solid electrolyte interface (SEI) for dendrite-free homogeneous Zn deposition [74]. The SEI layer prevents metallic Zn from contacting water and inhibits side reactions while providing a diffusion pathway for Zn^{2+}. This leads to a homogenization of the Zn^{2+} flux, as shown in Fig. 11b. However, studies on the electrode/electrolyte interface of aqueous zinc-ion battery systems have primarily focused on the surface of the zinc anode. This has been achieved through the construction of SEIs or the design of interfacial membranes with a uniform electric field and induced deposition to stabilize the zinc anode.

In contrast, there have been few reports on the influence of the interfacial properties of the electrolyte and anode on the cathode material. During the de/insertion process on the surface of the positive electrode, Zn^{2+} is accompanied by a significant amount of H^+/H_3O^+ co-embedding. This results in a notable change in the local pH at the electrode interface during charging and discharging, as depicted in Fig. 11c. The dissolution of the positive electrode material is exacerbated by this change, leading to the formation of by-products such as alkaline zincates [9,30,58,62,64]. To address this issue, Ren *et al.* introduced a new electrolyte containing $Zn(OTF)_2$ into a mixed solution of triethyl phosphate and water. This was done in order to prevent irreversible cathodic transformation and to increase the output voltage of the P-KVP cathode. The formation of a P-rich cathode electrolyte interfacial layer on the cathode surface was observed, which extended the cycle life [15]. However, current studies on aqueous batteries in a wide temperature range focus primarily on electrolyte design and negative electrode protection. The temperature sensitivity of cathode materials significantly affects the electrochemical performance of aqueous full batteries. High-temperature environments exacerbate self-discharge and dissolution problems of cathode materials, while low-temperature environments slow interfacial diffusion kinetics, both leading to rapid failure in battery performance (Fig. 11d) [18,20]. Electrode materials face different challenges in high and low temperature environments. At high temperatures, self-discharge and dissolution are issues, while at low temperatures, interfacial diffusion limitation and slow kinetics are problems. Designing materials that can address all of these challenges simultaneously is difficult. This presents a significant challenge for the development of wide-temperature-range cathode materials that can operate efficiently in both high and low-temperature environments.

In conclusion, the capacity of zinc-ion batteries may rapidly decay due to the dissolution of the positive and negative electrodes in the electrolyte. While severe zinc dendrite growth is not observed in zinc-ion batteries with neutral electrolytes at low current densities, the issue of dendrites cannot be overlooked at high current densities. In aqueous solutions, the presence of a large amount of free water makes side reactions, such as the dissolution of cathode active substances, corrosion of zinc anode, and generation of other products on the anode and cathode, unavoidable. Therefore, there is an urgent need to find new zinc salts and polymer crosslinking molecular additives at a reasonable price to adjust the concentration of the electrolyte for aqueous electrolytes. This will improve the interfacial properties of the positive and negative electrodes, widen the window of electrochemical stabilization, improve Coulombic efficiency, and prolong the stability of the battery cycle.

6. Summary and outlook

This paper describes the advantages of aqueous zinc-ion batteries, the energy storage mechanism, and the research progress of cathode and anode materials, along with corresponding modification strategies and potential improvements for the electrolyte. The research status of positive electrode materials, such as MnO_2, VO_2, and V_2O_5, is briefly summarized, and relevant modification studies are listed. Methods for improving zinc negative electrodes are proposed, addressing issues such as zinc dendrites, corrosion, hydrogen precipitation, and passivation. The article discusses the interfacial interaction between the electrolyte and the positive and negative electrode materials. It emphasizes the need for new zinc salts and additives to improve the interfacial properties of the electrolyte and the electrodes. Meanwhile, through continuous re-

search, the aqueous zinc-ion battery has shown promise due to its safety, low cost, and eco-friendliness. Finally, based on the above discussion, the next development of zinc-ion battery is prospected:

(1) Research and development of new cathode materials, focusing on cathode materials that provide both high voltage (>1.2 V) and large capacity (>400 mAh/g). To achieve high stability and high cyclability of electrodes for commonly used cathode materials, certain Mn^{2+} and Zn^{2+} are added. The most common modification methods include form-building engineering, interface modification engineering, defect/void engineering, and structural modulation engineering.
(2) Although the current optimization strategy for the zinc negative electrode does not perfectly solve the problems of dendrites and side reaction passivation, it indicates the future research direction for battery optimization. Research on improving battery performance by modifying the zinc electrode can be based on three major directions: Improving the structure of the zinc electrode by using functional materials or materials with porous or layered structures; adding additives to the electrolyte to optimize the structure or morphology of the electrode; and zinc alloying.
(3) The article discusses the challenges of safe use in aqueous zinc-ion batteries, specifically low-temperature solidification and electrolyte leakage. To address these issues, the electrolyte is changed from liquid to semi-solid/solid by adding polymer cross-linking molecules that reduce the electrolyte's low-temperature solidification point and high-temperature evaporation rate. This enhances the maintenance-free capability and wide-temperature range application potential of zinc-ion batteries.

Declaration of competing interest

The authors declare that they have no known competing financial interests or personal relationships that could have appeared to influence the work reported in this paper.

CRediT authorship contribution statement

Tong Peng: Writing – original draft. **Yupeng Xing:** Writing – original draft. **Lan Mu:** Writing – original draft. **Chenggang Wang:** Writing – original draft. **Ning Zhao:** Writing – original draft. **Wenbo Liao:** Writing – original draft. **Jianlei Li:** Writing – original draft, Funding acquisition. **Gang Zhao:** Writing – review & editing, Writing – original draft, Funding acquisition, Formal analysis.

Acknowledgments

This work was supported by the National Natural Science Foundation of China (No. U22A20140), the Jinan City-School Integration Development Strategy Project (No. JNSX2023015), Independent Cultivation Program of Innovation Team of Ji'nan City (No. 202333042), the University of Jinan Disciplinary Cross-Convergence Construction Project 2023 (No. XKJC-202309) and the Youth Innovation Group Plan of Shandong Province (No. 2022KJ095). Project supported by State Key Laboratory of Powder Metallurgy, Central South University, Changsha, China.

References

[1] X. Gu, J. Wang, X. Zhao, et al., J. Energy Chem. 85 (2023) 30–38.
[2] Y. Zong, H. He, Y. Wang, et al., Adv. Energy Mater. 13 (2023) 2300403.
[3] S. Yang, Y. Li, H. Du, et al., ACS Sustain. Chem. Eng. 10 (2022) 12630–12641.
[4] H.R. Kim, Y. Ji, Y. Chun, et al., Mater. Today Sustain. 23 (2023) 100456.
[5] D. Luo, J. Wu, X. Chi, Y. Liu, ACS Appl. Energy Mater. 6 (2023) 3705–3713.
[6] K.E.K. Sun, T.K.A. Hoang, T.N.L. Doan, et al., ACS Appl. Mater. Interfaces 9 (2017) 9681–9687.
[7] T. Mageto, S.D. Bhoyate, K. Mensah-Darkwa, A. Kumar, R.K. Gupta, J. Energy Storage 70 (2023) 108081.
[8] Y. Zeng, H. Wang, M. Rauf, et al., Electrochim. Acta 447 (2023) 142085.
[9] W. Zheng, H. Xie, L. Zhu, H. Zhou, K. Zhang, J. Energy Storage 76 (2024) 109808.
[10] Z. Peng, Y. Li, P. Ruan, et al., Coord. Chem. Rev. 488 (2023) 215190.
[11] A. Duan, S. Luo, W. Sun, Chin. Chem. Lett. 35 (2024) 108337.
[12] X. Wang, Z. Zhang, B. Xi, et al., ACS Nano 15 (2021) 9244–9272.
[13] D. Zhu, J. Li, F. Ren, et al., J. Colloid Interface Sci. 651 (2023) 504–513.
[14] L. Zhang, H. Guo, W. Zong, et al., Energy Environ. Sci. 16 (2023) 4872–4925.
[15] L. Wang, M. Zhao, X. Zhang, et al., J. Energy Chem. 93 (2024) 71–78.
[16] Y. Zong, H. Chen, J. Wang, et al., Adv. Mater. 35 (2023) 2306269.
[17] Y.L. Li, S. Lin, D.F. Sun, Z.Q. Lei, Acta Chim. Sin. 79 (2021) 200–207.
[18] J. Zheng, C. Qin, C. Chen, et al., J. Mater. Chem. A 11 (2023) 24311–24320.
[19] R. Rehman, X. Zhang, M. Chang, et al., ACS Omega 7 (2022) 33942–33948.
[20] C. Xie, S. Liu, H. Wu, et al., Sci. Bull. 68 (2023) 1531–1539.
[21] D. Wang, W. Liang, X. He, et al., ACS Appl. Mater. Interfaces 15 (2023) 20876–20884.
[22] Y. Zuo, T. Meng, H. Tian, et al., ACS Nano 17 (2023) 5600–5608.
[23] Q. Yang, Y. Chen, Y. Yang, et al., Ind. Eng. Chem. Res. 62 (2023) 16757–16765.
[24] Q. Feng, Y. Cao, C. Guo, et al., ACS Appl. Energy Mater. 6 (2023) 7899–7907.
[25] C. Zhong, B. Liu, J. Ding, et al., Nat. Energy 5 (2020) 440–449.
[26] Y. Huang, J. Mou, W. Liu, et al., Nano-Micro Lett. 11 (2019) 49.
[27] Y.F. Huang, T. Gu, G. Rui, et al., Energy Environ. Sci. 14 (2021) 6021–6029.
[28] F. Li, H. Sheng, H. Ma, et al., ACS Appl. Energy Mater. 6 (2023) 6201–6213.
[29] C. Yin, J. Chen, C.L. Pan, Y. Pan, J. Hu, ACS Appl. Energy Mater. 5 (2022) 14144–14154.
[30] B. Lee, H.R. Seo, H.R. Lee, et al., ChemSusChem 9 (2016) 2948–2956.
[31] C.C. Kao, C. Ye, J. Hao, et al., ACS Nano 17 (2023) 3948–3957.
[32] O. Buyukcakir, R. Yuksel, F. Begar, et al., ACS Appl. Energy Mater. 6 (2023) 7672–7680.
[33] Z. Sang, J. Liu, X. Zhang, et al., ACS Nano 17 (2023) 3077–3087.
[34] X. Geng, Y. Jiang, H. Ma, et al., ACS Appl. Mater. Interfaces 14 (2022) 49746–49754.
[35] K.W. Nam, S.S. Park, R. dos Reis, et al., Nat. Commun. 10 (2019) 4948.
[36] Y. Ru, S. Zheng, H. Xue, H. Pang, Mater. Today Chem. 21 (2021) 100513.
[37] S. Li, M. Zhao, D. Zhang, X. Wu, Cryst. Growth Des. 23 (2023) 8156–8162.
[38] S. Xin, X. Dong, D. Jin, L. Yang, D. Su, J. Alloys Compd. 968 (2023) 172115.
[39] M.H. Alfaruqi, V. Mathew, J. Gim, et al., Chem. Mater. 27 (2015) 3609–3620.
[40] C. Wang, Y. Zeng, X. Xiao, et al., J. Energy Chem. 43 (2020) 182–187.
[41] S. Mallick, V.S.K. Choutipalli, S. Bag, V. Subramanian, C.R. Raj, ACS Appl. Mater. Interfaces 14 (2022) 37577–37586.
[42] D. Wu, S.T. King, N. Sadique, et al., J. Mater. Chem. A 11 (2023) 16279–16292.
[43] X. Yang, Z. Jia, W. Wu, et al., Chem. Commun. 58 (2022) 4845–4848.
[44] H. Yang, D. Chen, R. Zhao, et al., Energy Environ. Sci. 16 (2023) 2910–2923.
[45] L. Zhao, Y. Tan, Y. Sun, et al., J. Electroanal. Chem. 944 (2023) 117636.
[46] Y. Wang, S. Zhang, Y. Zhang, et al., Electrochim. Acta 475 (2024) 143623.
[47] J. Chen, B. Xiao, C. Hu, et al., ACS Appl. Mater. Interfaces 14 (2022) 28760–28768.
[48] L. Chen, Z. Yang, Y. Huang, Nanoscale 11 (2019) 13032–13039.
[49] K. Muthukumar, S. Rajendran, A. Sekar, Y. Chen, J. Li, ACS Sustain. Chem. Eng. 11 (2023) 2670–2679.
[50] S. Zhao, G. Tian, D. Zhang, Q. Wang, ACS Appl. Nano Mater. 6 (2023) 1849–1858.
[51] K. Li, Y. Liu, X. Wu, ACS Appl. Nano Mater. 6 (2023) 12439–12446.
[52] M. Wu, C. Shi, J. Yang, et al., Adv. Mater. 36 (2024) 2310434.
[53] C. Li, J. Zhang, K. Zhang, et al., ACS Sustain. Chem. Eng. 11 (2023) 15470–15479.
[54] C. Yang, S. Ding, Y. Zhao, et al., Dalton Trans. 52 (2023) 16984–16992.
[55] J. Xiang, M. Luo, X. Wu, et al., Chem. Commun. 58 (2022) 9104–9107.
[56] K. Xhanari, M. Finšgar, Analyst 148 (2023) 5805–5821.
[57] X. Zhang, T. Liao, T. Long, et al., ACS Appl. Mater. Interfaces 15 (2023) 32496–32505.
[58] H. Sun, Y. Huyan, N. Li, et al., Nano Lett. 23 (2023) 1726–1734.
[59] H. Wang, J. Huang, X. Wang, Z. Guo, W. Liu, ACS Appl. Mater. Interfaces 15 (2023) 20541–20550.
[60] Y.J. Kwon, M.G. Jung, B.U. Yoo, H.S. Park, ACS Appl. Energy Mater. 6 (2023) 4748–4756.
[61] X. Zhang, Q. Ruan, L. Liu, et al., J. Electroanal. Chem. 936 (2023) 117357.
[62] S. Kim, G.H. Ryu, G.H. An, Appl. Surf. Sci. 635 (2023) 157634.
[63] Y. Liang, F. Kong, Z. Wang, et al., J. Alloys Compd. 936 (2023) 168378.
[64] X. Li, P. Ye, A. Dou, et al., J. Energy Storage 76 (2024) 109874.
[65] N. Yu, Y. Li, W. She, et al., ACS Appl. Mater. Interfaces 14 (2022) 50827–50835.
[66] L. Sha, B.B. Sui, P.F. Wang, et al., Chem. Eng. J. 481 (2024) 148393.
[67] H. Li, C. Xu, C. Han, et al., J. Electrochem. Soc. 162 (2015) A1439.
[68] L. Yan, X. Zeng, Z. Li, et al., Mater. Today Energy 13 (2019) 323–330.
[69] X. Yuan, C. He, J. Wang, et al., J. Alloys Compd. 970 (2024) 172523.
[70] S. Xie, Y. Li, L. Dong, J. Energy Chem. 76 (2023) 32–40.
[71] Z. Qi, T. Xiong, Z.G. Yu, et al., J. Power Sources 558 (2023) 232628.
[72] Q. Zhang, Y. Ma, Y. Lu, et al., Nat. Commun. 11 (2020) 4463.
[73] N. Wang, Y. Zhang, J. Yuan, et al., ACS Appl. Mater. Interfaces 14 (2022) 48081–48090.
[74] X. Li, J. Miao, F. Hu, et al., J. Mater. Chem. A 12 (2024) 968–978.